

Significant decrease of the lattice thermal conductivity due to phonon confinement in a free-standing semiconductor quantum well

Alexander Balandin and Kang L. Wang

Device Research Laboratory, Electrical Engineering Department, University of California—Los Angeles, Los Angeles, California 90095-1594

(Received 17 February 1998; revised manuscript received 20 April 1998)

Lattice thermal conductivity of a quantum well limited by umklapp, impurity, and boundary scattering was investigated theoretically by taking into account dispersion of confined acoustic-phonon modes. We show that strong modification of phonon group velocities due to spatial confinement leads to a significant increase in the phonon relaxation rates. From the numerical calculations, we predict a decrease by an order of magnitude of the lattice thermal conductivity in a 100-Å-wide free-standing quantum well. Our theoretical results are consistent with recent experimental investigations of the lateral thermal conductivity of nitride/silicon/oxide membranes conducted in our group. [S0163-1829(98)00928-X]

I. INTRODUCTION

Thermal properties of semiconductor nanostructures and superlattices have recently attracted a lot of attention. This is primarily due to two major factors. The first one is a continuous scaling down of the feature sizes in microelectronic devices and circuits, which leads to an increase in power dissipation per unit area of the semiconductor chip. Under such conditions, the influence of size effects on thermal conductivity becomes extremely important for device design and reliability.¹ The problem of thermal management is even more severe for photonic devices such as vertical cavity surface emitting lasers, in which the heat generation density reaches 10^6 W/cm³. The second factor is a rebirth of the field of thermoelectric materials, which has been brought about by the emergence of large numbers of new artificially synthesized materials, including those structured on an atomic scale.² In order to dissipate the increasing amount of heat from the chip area, one has to engineer material parameters or structure geometry in such a way that thermal conductivity is large along particular directions. To improve performance of thermoelectrics, one needs to achieve low thermal conductivity. These are two contradictory demands, but both can be approached with appropriate modification of phonon modes, e.g., phonon engineering.

The quest for superior thermoelectric materials generally requires finding conditions such that the thermoelectric figure of merit $ZT = S^2 \sigma T / (\kappa_l + \kappa_e)$ (where S is the Seebeck coefficient, σ is the electrical conductivity, κ_l is the lattice thermal conductivity, κ_e is the electronic thermal conductivity, and T is absolute temperature) is as large as possible. Recent reports that predicted strong enhancement of the figure of merit³⁻⁶ for semiconductor superlattices and quantum wells treated rigorously only electronic contribution κ_e while ignoring the effects of spatial confinement on κ_l . However, a smaller value of κ_l would lead to even further increase of ZT .

It was shown earlier that phonon transport in superlattices can be significantly modified due to formation of minibands and emergence of the mini-umklapp process, a new type of

umklapp scattering processes associated with transitions between the mini-Brillouin zones.^{7,8} A dramatic suppression of the perpendicular thermal transport in superlattices at high temperatures was also predicted in Ref. 9. In the structures considered in Refs. 7 and 8, the modification of phonon transport comes from the periodicity (additional to the crystal lattice periodicity) in the direction of superlattice layering. In such a case, the minireciprocal lattice vectors associated with superlattice minizones give rise to mini-umklapp processes that contribute to the thermal resistance.⁷ The situation is quite different in single quantum wells, which are either free standing or embedded into material with distinctively different elastic properties. Here, the phonon dispersion changes due to the phonon spatial confinement induced by the boundaries. This affects all phonon relaxation rates, and makes the thermal transport properties of quantum wells rather different from those of superlattices. In this paper, we address the issue of how *spatial confinement of acoustic phonon modes directly modifies the lateral lattice thermal conductivity* in a free-standing quantum well.

Recently, some of us reported the results of experimental investigation of the lateral thermal conductivity of nitride/silicon/oxide membranes measured with a suspended microstructure.¹⁰ An extremely large reduction of κ_l (more than an order of magnitude) was observed in the temperature range from $T = 293$ to 413 K. Such a huge drop in thermal conductivity cannot be attributed entirely to boundary scattering and structure imperfections, and is likely to be related to modification of phonon modes and corresponding change in the thermal transport. The geometry of the structure, material parameters, and temperature regime used in our model approximately correspond to the conditions of the experiment. The results of numerical simulations presented below were obtained for a free-standing quantum well since the boundary conditions for the elasticity equation are the simplest in this case. But the model can be easily extended to include quantum wells embedded into rigid materials by proper modification of the boundary conditions. Qualitatively, the change due to different boundaries will be discussed below.

The rest of the paper is organized as follows. In the next

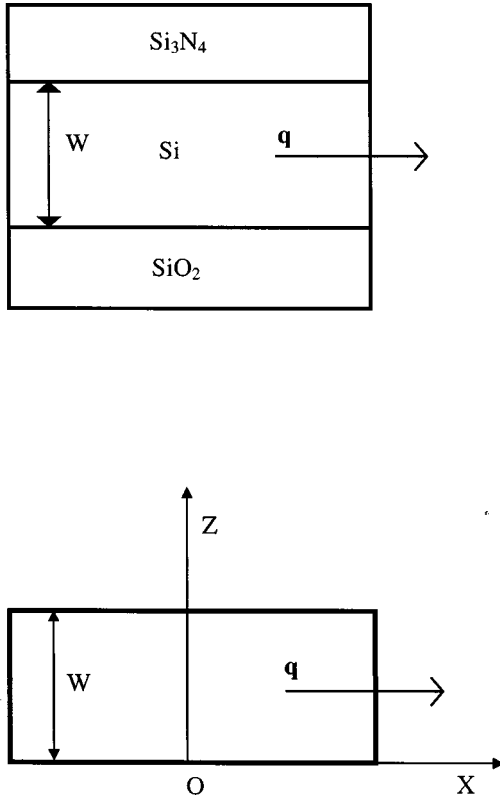


FIG. 1. Geometry of the structure used for model simulations (lower part). Geometry of the experimental structure (upper part).

section we describe the calculation of the lattice thermal conductivity, which takes into account modification of the acoustic-phonon dispersion due to spatial confinement. The model is based on the proper modification of the corresponding bulk formulas and phonon group velocities obtained from the continuous medium approximation with specific boundary conditions. It also takes into account new selection rules for three-phonon umklapp processes imposed by the emergence of additional phonon dispersion branches. In Sec. III, we present the results of numerical simulations. Confinement of acoustic phonons and corresponding change in their group velocity lead to an increase in the phonon relaxation rates and, thus to the drop in thermal conductivity. Discussion and comparison of the theoretical results with available experimental data are given in Sec. IV. We present our conclusions in Sec. V.

II. THEORY

A. Calculation of the thermal conductivity

We consider a generic quantum well structure (see Fig. 1) at relatively high temperatures so that three-phonon interaction is expected to be the dominant scattering mechanism limiting heat transfer. The electronic contribution κ_e is assumed to be small in undoped fully depleted semiconductor structures, and will be neglected in our calculations. It is well known that the normal three-phonon scattering processes (N processes) in which the total momentum is conserved cannot by themselves lead to a finite thermal resistance, although they influence it indirectly by redistributing phonon modes.^{11,12} Only processes that do not conserve crystal mo-

mentum contribute to the lattice thermal resistance. Such processes, further referred to as resistive, are boundary scattering, impurity scattering, and the three-phonon umklapp scattering process (U process), in which the sum of phonon wave vectors is not conserved but changes by a reciprocal-lattice vector \mathbf{G} . Impurity scattering, in its turn, can be separated for isotope scattering arising from the presence of atoms with different mass, dislocation scattering, and scattering on atoms of different elements. In a high-quality material, all of these impurity scattering mechanisms can be strongly reduced except for the isotope scattering. For this reason, we will be primarily interested in examining the effects produced by phonon confinement on the resistive processes, which include the three-phonon umklapp processes, isotope scattering, and boundary scattering.

In order to calculate κ_l , we use Callaway's expression for the thermal conductivity under the assumption that the resistive processes are dominant,¹¹

$$\kappa_l = \frac{k_B}{2\pi^2 v} \left(\frac{k_B}{\hbar} \right)^3 T^3 \int_0^{\theta/T} \frac{\tau_C x^4 e^x}{(e^x - 1)^2} dx, \quad (1)$$

where k_B is the Boltzmann constant, \hbar is the Planck constant, θ is the Debye temperature, $x = \hbar\omega/k_B T$, τ_C is the combined relaxation time, and v is the velocity of sound. Limiting our consideration to only three major contributions to the resistive process, we can write the following relation:

$$\frac{1}{\tau_C} = \frac{1}{\tau_U} + \frac{1}{\tau_B} + \frac{1}{\tau_I}, \quad (2)$$

where τ_U , τ_B , and τ_I are the relaxation times due to the U processes (all allowed channels), boundary scattering, and impurity scattering, respectively. As it will become clear later, all relaxation times are affected by the phonon confinement.

From the first-order perturbation theory, the single-mode relaxation rate of the U process for a thermal mode \mathbf{q} can be written as^{12,13}

$$\frac{1}{\tau_U} = \sum_{\mathbf{q}'} 2|C_3|^2 \frac{\hbar}{M^3 \omega \omega' \omega''} \frac{1 - \cos \Delta\omega t}{\Delta\omega^2 t} (N_0' - N_0''), \quad (3)$$

where $\Delta\omega = \omega + \omega' - \omega''$, $|C_3|^2 = (4\gamma^2/3n_a)(M^2/v^2)\omega^2\omega'^2\omega''^2$, n_a is the number of atoms per unit volume, M is the atomic mass, γ is the Grüneisen parameter, $N_0' \equiv N_0(\omega')$ and $N_0'' \equiv N_0(\omega'')$ are the equilibrium occupancies of modes \mathbf{q}' and \mathbf{q}'' , respectively, and the resonance factor defined by $(1 - \cos \Delta\omega t)/\Delta\omega^2 t \approx \pi\delta(\Delta\omega)$ ensures that the only significant contribution comes from frequencies for which $\Delta\omega = \omega + \omega' - \omega'' = 0$. The summation over \mathbf{q}' for each polarization branch can be approximated by $\sum_{\mathbf{q}'} \approx \nu(na^3/(2\pi)^3) \int dq' \int dS'$, where ν is the number of polarizations of the interacting mode \mathbf{q}' , a is the lattice constant, and S' is the locus of \mathbf{q}' satisfying the restriction $\Delta\omega = 0$. The equilibrium occupancy is given by the usual Planck distribution $N_0 = 1/[\exp(\hbar\omega/k_B T) - 1]$. We can rewrite Eq. (3) in the following form:

$$\frac{1}{\tau_U} \approx \frac{\nu \gamma^2 \hbar}{3 \pi^2 \rho v^2} \int_{q'} dS' \int \frac{d\Delta\omega}{v_g} \omega \omega' \omega'' \delta_i(\Delta\omega) \times (N_0(\omega') - N_0(\omega'')), \quad (4)$$

where $\Delta\omega = \omega + \omega' - \omega''$, ρ is the density of the crystal, $v_g = |\partial\Delta\omega/\partial q'|_n$ is the group velocity perpendicular to surface S' . In order to evaluate relaxation rates of Eq. (4), we should use the actual dispersion relations and group velocities, $v_g \equiv v_g(\omega(q))$, for phonons in a quantum well. The modification of wave vector selection and frequency conservation rules due to the spatial confinement should also be taken into account. Evaluation of the single-mode relaxation rate of the mode q , requires the integration over all possible q' modes. Details of calculation of $v_g(\omega(q))$ and $1/\tau_U$ are given in the next two sections.

The impurity scattering mechanism, which is most affected by spatial confinement through the group velocity, is the so-called isotope scattering arising from the presence of atoms with different mass. The relaxation time for this type of impurity scattering was given by Klemens as¹²

$$\frac{1}{\tau_I} = \frac{V_0 \omega^4}{4 \pi v_g^3} \Gamma = \frac{V_0 \omega^4}{4 \pi v_g^3} \sum_i f_i [1 - (M_i/M)]^2, \quad (5)$$

where V_0 is the volume per atom, M_i is the mass of an atom, f_i is the fractional content of atoms with mass M_i , which is different from M .

The relaxation time for the boundary scattering can be evaluated from the semiempirical relation^{12,14}

$$\frac{1}{\tau_B} = \frac{v_g}{W}, \quad (6)$$

where W is some characteristic thickness of a bulk semiconductor or the width of a quantum well. More precise description of the boundary scattering can be obtained using the approach of Ref. 1, which takes into account effects induced by partially diffuse and partially specular interfaces and boundaries. Equations (3)–(5) were derived for bulk and cannot be applied for strictly 2D systems since in this case a reduced zone picture and the umklapp formalism do not work in the growth direction. In our calculations we will consider rather thick quantum wells (many atomic layers) so that the formulas can still be applied.

B. Phonon dispersion and group velocities

Confined phonon modes can be calculated using the elasticity equation^{15–17}

$$\frac{\partial^2 \mathbf{u}}{\partial t^2} = s_l^2 \nabla^2 \mathbf{u} + (s_l^2 - s_t^2) \text{grad div } \mathbf{u}, \quad (7)$$

where \mathbf{u} is the displacement vector, and s_l and s_t are the speeds of longitudinal and transverse acoustic waves in the bulk. For Si, $s_l = 9.04 \times 10^5$ cm/s and $s_t = 5.34 \times 10^5$ cm/s. The normal components of the stress tensor on the free-standing quantum well must vanish. These boundary conditions, substituted instead of *periodic boundary conditions* of the bulk material, bring about a significant change to the

phonon dispersion and group velocities. One should note here that a significant modification of phonon modes can be attained not only in a free-standing quantum well but also in a quantum well embedded in rigid material (Si_3N_4 and SiO_2 , for example) or in a heterostructure with relatively large difference of lattice constants. In the case of a quantum well embedded in rigid material, the normal components of the stress tensor are unrestricted but the displacement \mathbf{u} is zero at the boundary. This corresponds to the clamped-surface boundary conditions.¹⁷

There are three different types of confined acoustic modes in a quantum well characterized by their distinctive symmetries:¹⁵ shear (S) waves, dilatational (D) waves, and flexural (F) waves. The S modes are similar to the transverse (T) modes in bulk semiconductor and have only one nonzero component of the displacement vector $\mathbf{u} = (0, u_y, 0)$, which is perpendicular to the direction of wave propagation, $\mathbf{q}_{\parallel} = (q_x, 0)$, and lies in the plane of the quantum well. The dispersion relation for the S modes can be written as $\omega_n = s_t \sqrt{q_x^2 + q_{z,n}^2}$, where subscript n denotes different branches of the same polarization type, and the $q_{z,n}$ is quantized as $q_{z,n} = \pi n/W$. The D and F phonon modes have two nonzero components $\mathbf{u} = (u_x, 0, u_z)$ with dispersion relation given by $\omega_n = s_l \sqrt{q_x^2 + q_l^2}$ where the set of parameters q_l defines different branches of the same polarization denoted by subscript l . Since these types of confined waves have a component in the direction of propagation, they can be viewed as a modification of the bulk longitudinal (L) mode.

III. NUMERICAL RESULTS

Solving numerically Eq. (7), we first find confined phonon modes for a particular well width and material parameters and then, by numerical differentiation, determine the group velocities. The phonon group velocity in the n th branch is defined as $v_g^{(n)} = \partial\omega_n/\partial q$. The dispersion relation for the phonon S and D modes are shown in Fig. 2 for a 10-nm-wide Si quantum well. Corresponding group velocities for the S and D modes are presented in Fig. 3. It is easy to see that there are more dispersion and velocity branches for each polarization type as compared to the bulk, and group velocities of all branches decrease. The higher the mode number the smaller the group velocity so that for thermal modes the decrease in group velocities is up to 3–4 times.

The change of polarization types and the $\omega \equiv \omega(q)$ dependence brings also modifications of the energy and momentum conservation laws. It is known that for isotropic semiconductors only two general types of processes are allowed:^{12,18} $T + T \leftrightarrow L$, or $L + T \leftrightarrow L$. This restriction follows from the requirement that (i) all three interacting modes cannot belong to the same polarization branch, and (ii) the resultant mode should be above two initial (interacting) modes. It turns out that for confined acoustic phonons, the D mode is almost always above the S mode corresponding to the same branch n (see Fig. 2). Comparing dispersion on Figs. 2(a) and 2(b), one can see that only for a small fraction of phonons with in-plane wave vectors close to the zone center ($q_x < 0.5 \text{ nm}^{-1}$), some branches n' of the D mode may have a smaller energy than that of the corresponding S mode. Thus, the processes $D_n + S_n \leftrightarrow D_n$ and $S_n + S_n \leftrightarrow D_n$

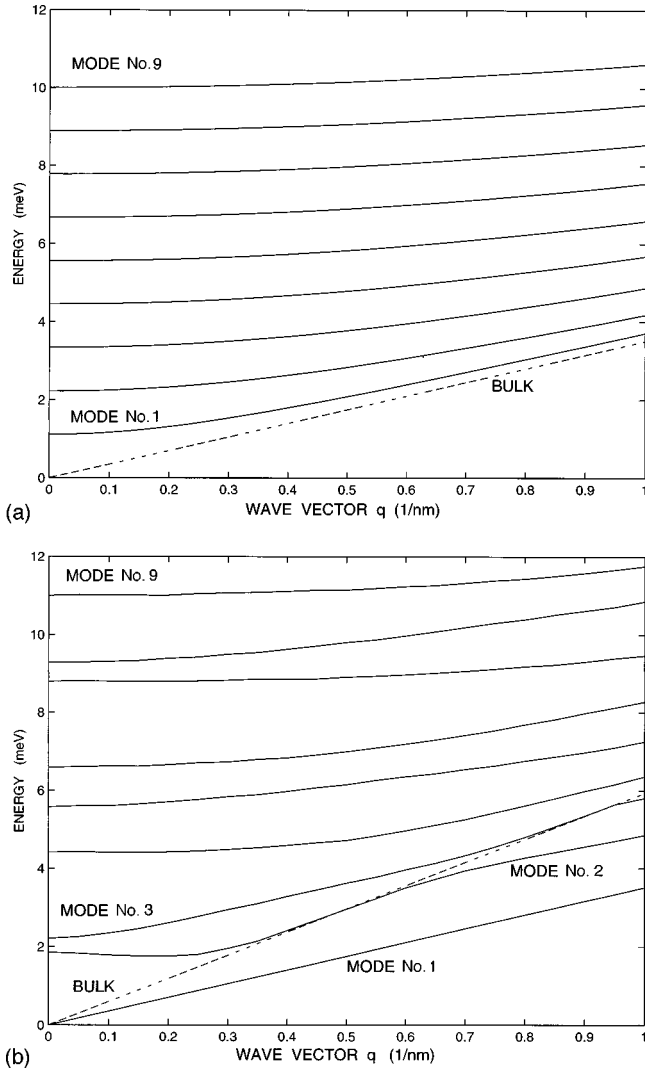


FIG. 2. Dispersion relation for the shear (a) and dilatational (b) modes in a 10-nm-wide silicon quantum well. The dashed lines show the dispersion relation for the bulk transverse (a) and longitudinal (b) acoustic-phonon modes.

are *allowed* and can be treated by analogy with the bulk processes $L+T \leftrightarrow L$ and $T+T \leftrightarrow L$, respectively. In our model calculations we have neglected the S and D mode intermixing for the n' branches close to the zone center. More precise treatment would require separation of the frequency range where the S mode is higher in energy than the D mode, and considering $D_{n'} + S_{n'} \leftrightarrow S_{n'}$ as an allowed process.

In order to obtain the scattering rate for the U process that goes through all possible channels, we write Eq. (4) for each of these channels, substitute dispersion relation and group velocity calculated for the relevant range of q , and then sum all together. As an example, we show how to estimate the relaxation rate for a dilatational mode of frequency $\omega_D(q)$ in the scattering process that goes through the channel $D+S \leftrightarrow D$. Following the derivation in Ref. 13, we assume in Eq. (4) that frequencies $\omega' \approx \omega_S$ and $\omega'' \approx \omega_D(q) + \omega_S$. We use the calculated dispersion for $\omega_D(q)$ over the relevant

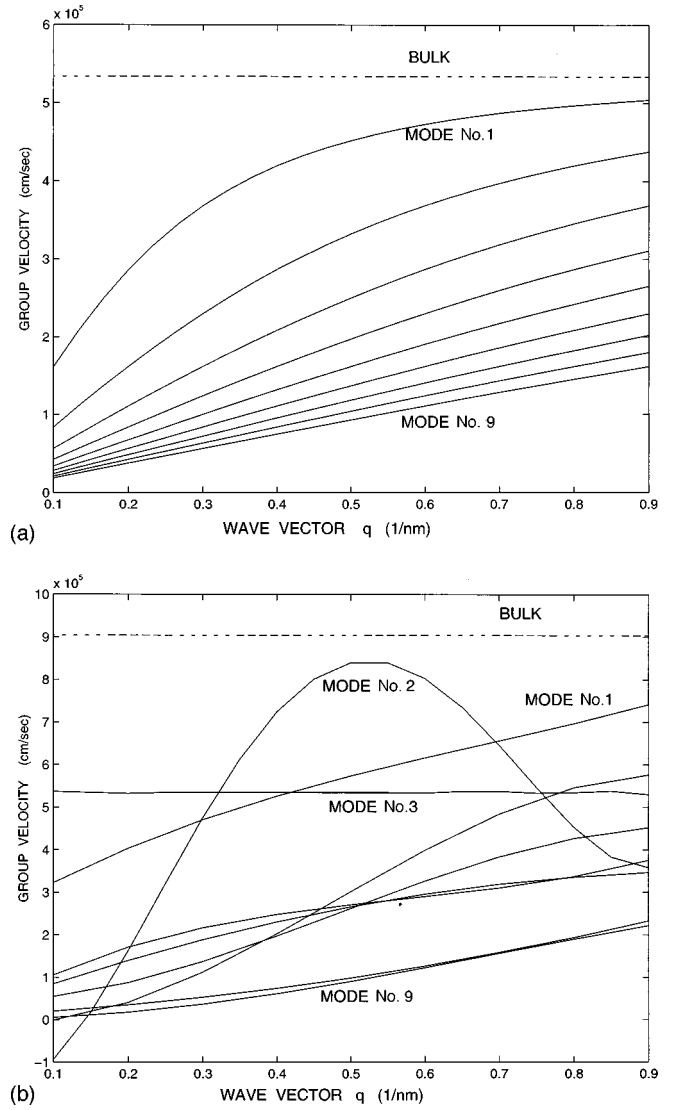


FIG. 3. Group velocity as a function of the in-plane wave vector for the shear (a) and dilatational (b) modes in a 10-nm-wide silicon quantum well. The dashed lines show the group velocity for the bulk transverse (a) and longitudinal (b) acoustic phonon modes, respectively.

range of q , and ω_S at the zone boundary. Thus, the relaxation rate can be written as

$$\frac{1}{\tau_U} \approx \frac{v\gamma^2 \hbar \omega_D(q) \omega_S [\omega_D(q) + \omega_S]}{3\pi^2 \rho v^2 v_g} \times \left(\frac{1}{e^{\hbar\omega_S/k_B T} - 1} - \frac{1}{e^{\hbar[\omega_D(q) + \omega_S]/k_B T} - 1} \right) \int_{q'} dS'. \quad (8)$$

Here the integration over surface S' is being carried out the same way as in Ref. 13. One can note in Eq. (8) that the relaxation rate is positively defined since $\omega_D(q) + \omega_S > \omega_S$. The latter holds for all allowed channels. In our calculation we neglect optical phonon modes since for Si, particularly in

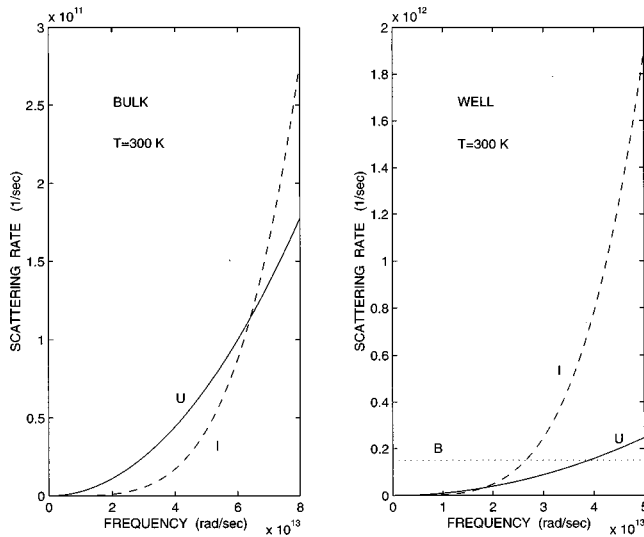


FIG. 4. Phonon relaxation rates due to different scattering mechanisms as functions of phonon frequency ($\omega \approx 4 \times 10^{13}$ rad/sec is a thermal mode at $T=300$ K). The left panel corresponds to the bulk material while the right panel to the quantum well. The relaxation rates due to the umklapp (U), impurity (I), and boundary (B) scattering processes are depicted. Note the change in scale.

$\langle 110 \rangle$ direction, their contribution in thermal transport is less significant than that one of the confined acoustic phonon modes. Although, for some material systems (like LiF or NaF), the optical dispersion curve intercepts all longitudinal bulk modes in all directions — $\langle 100 \rangle$, $\langle 110 \rangle$, $\langle 111 \rangle$ — and thus has to be included. Since optical phonon modes are not significantly affected by spatial confinement, the situation in quantum wells is not expected to be different from the bulk.

Finally, we evaluate phonon scattering rates using Eqs. (5)–(8) for a bulk Si 10- μm -thick slab and Si 10- and 155-nm-wide quantum wells. The material parameters used in simulation were the following: $a = 5.45 \text{ \AA}$, $\rho = 2.42 \times 10^3 \text{ kg/m}^3$, $M = 46.6 \times 10^{-27} \text{ kg}$, $n_a \approx 7.3$, $\gamma = 0.56$, $\theta = 625 \text{ K}$, and $\Gamma \times 10^4 = 2.64$ for three Si isotopes.¹⁹ The relaxation rates due to different scattering mechanisms are shown in Fig. 4 as functions of phonon frequency. In the case of bulk material, the U process is a dominant scattering mechanism over almost the entire frequency range which is important for Si (from 1.80×10^{13} to 6.06×10^{13} rad/sec). The latter is expected at high temperatures. The scattering rate due to boundaries is not shown since it is two orders of magnitude smaller than shown rates for a given slab thickness. For a quantum well, the impurity scattering rate that is proportional to ω^4 takes the lead at frequencies above 2.5×10^{13} rad/sec. The dominant mechanism at low frequencies is the boundary scattering. The overall scattering rate increases in a quantum well. One important thing to note is that by improving crystal and surface quality one can reduce the impurity and boundary scattering rates but not the umklapp scattering rate. The increase of the U -process scattering rate in a quantum well is a direct result of the modification of phonon dispersion due to spatial confinement of the phonon modes. The latter leads to the reduction of the group velocity, which also strongly increases the impurity scattering as it is proportional to $1/v_g^3$.

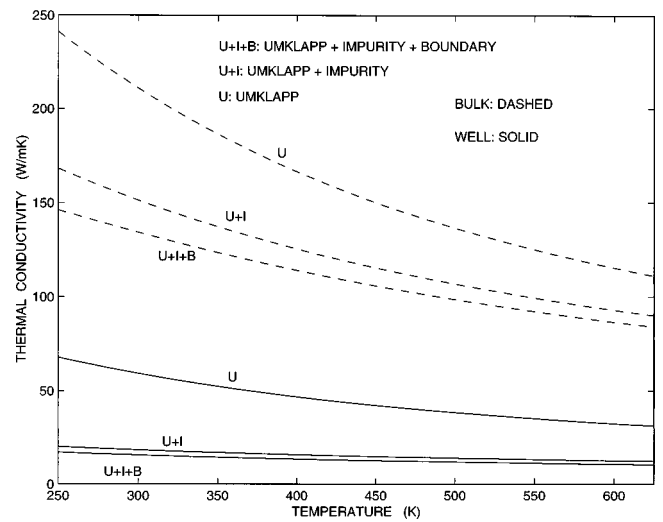


FIG. 5. Lattice thermal conductivity as a function of temperature for bulk material (dashed) and the quantum well (solid). Each case is illustrated by three curves that correspond to the thermal conductivity limited by the umklapp scattering only (U), the umklapp and impurity scattering only ($U+I$), and by all processes including boundary scattering ($U+I+B$).

IV. DISCUSSION

In Fig. 5 we show the lattice thermal conductivity as a function of the temperature for the quantum well and the bulk material. In order to illustrate the contribution of different scattering mechanisms to the thermal resistivity, the conductivities limited only by the umklapp scattering and by the umklapp and impurity scattering are also shown. The umklapp limited conductivity drops about 3.5 times because of spatial confinement of phonons. The overall thermal conductivity of a quantum well at 300 K is about 13% of the bulk Si.

The calculated value and temperature dependence of the thermal conductivity are consistent with the results of the experimental investigation recently reported by some of us.¹⁰ The measurements were conducted with a suspended microstructure which served as a thermal bridge using the differential and equivalent circuit methods. These measurements have shown that the lateral thermal conductivity of a Si_3N_4 (150 nm)/monocrystalline Si(155 nm)/ SiO_2 (300 nm) structure was about 1.5% of the conductivity of the bulk Si and was almost a constant in the temperature range from $T = 293$ to 413 K. The total error for the measurements was estimated to be less than 20%. Although our model assumed a free-standing quantum well, the results can be extended to quantum wells with rigid boundaries. The lowest confined phonon modes in a quantum well with clamped-surface boundary conditions are higher in energy than those in a free-standing quantum well, but the overall behavior and the decrease of the group velocities are very similar in both cases. The model presented here can be developed further to include mixed boundary conditions and interface quality. Our model applied to a 155-nm-wide Si well gives $k_l = 66.7 \text{ W/m K}$. For comparison, experimentally measured thermal conductivity of bulk Si is 148 W/m K. This is a significant drop although much less than that observed in the experiment. The temperature dependence of the calculated k_l

is very close to the measured one. The discrepancy in our calculated and measured values of k_l may be attributed to (i) underestimated in our model boundary scattering, (ii) the presence of other defect scattering processes (like scattering on dislocations), or (iii) crystal anisotropy, strain effects, and related phonon focusing.

Our results are in excellent agreement with the most recent data reported in Ref. 20. In Ref. 20, the authors predicted a significant reduction of the in-plane lattice thermal conductivity for Si layers thinner than $0.2 \mu\text{m}$ at temperatures as high as 700 K. In accordance with their model, the thermal conductivity of a $0.05 \mu\text{m}$ pure Si film at 400 K in silicon-on-insulator structures is about 30% of the bulk value. Although their theoretical approach is different from ours and it is applied to thicker Si layers, the obtained results confirm our own conclusions. Our results are also in line with experimental data presented in Ref. 21. It was reported there that the lattice thermal conductivity of the $\text{Bi}_{0.5}\text{Sb}_{1.5}\text{Te}_3$ films is considerably lower than k_l of bulk crystals of the same solid solution. The experimentally observed temperature dependence in Ref. 21 is very close to the one calculated on the basis of our model. Further experiments and calculations are needed in order to completely clarify the physics of extremely low thermal conductivity of semiconductor quantum wells with free-surface or rigid boundaries. A possible experimental verification of the phonon confinement nature of the observed drop in the thermal conductivity can be an observation of substantial dependence of k_l on quantum well thickness. An absence of such dependence would be an indication that the decrease is mostly due to phonon scattering from boundary imperfection. Such work is currently in progress.²²

V. CONCLUSIONS

We have presented a study of the effects of phonon spatial confinement on the lateral lattice thermal conductivity of semiconductor quantum wells with free-surface boundaries. It was shown that strong modification of the phonon dispersion and group velocities due to spatial confinement leads to a significant increase of the relaxation rates in three-phonon umklapp scattering, impurity scattering, and boundary scattering processes. From the numerical calculations we predict a strong decrease of the lattice thermal conductivity of a quantum well (13% of the bulk value for a 10-nm-wide well). Our theoretical results favorably agree with the recent experimental investigation of the lateral thermal conductivity of a 155-nm-wide Si quantum well. Modification of the lattice thermal conductivity by confined phonon modes opens up a novel tuning capability of thermoelectric properties of heterostructures, and may lead to a strong increase of ZT in specially designed semiconductor nanostructures.

ACKNOWLEDGMENTS

The authors acknowledge very helpful discussions on confined phonon modes with Professor V. Mitin, Professor G. Chen, and Dr. A. Svizhenko. The authors thank Dr. X. Y. Zheng for comments regarding experimentally measured thermal conductivity. This work was supported by the DoD MURI-ONR program on Thermoelectrics (Dr. John Pazik) and DoD MURI-ARO program on Low Power Electronics (Dr. James Harvey).

-
- ¹C. L. Tien and G. Chen, *J. Heat Transfer* **116**, 799 (1992); G. Chen, *ibid.* **119**, 220 (1997).
- ²G. Mahan, B. Sales, and J. Sharp, *Phys. Today* **50** (3), 42 (1997).
- ³J. O. Sofo and G. D. Mahan, *Appl. Phys. Lett.* **65**, 2690 (1994); G. D. Mahan and H. B. Lyon, Jr., *J. Appl. Phys.* **76**, 1899 (1994).
- ⁴L. D. Hicks and M. S. Dresselhaus, *Phys. Rev. B* **47**, 12 727 (1993).
- ⁵L. D. Hicks, T. C. Harman, and M. S. Dresselhaus, *Appl. Phys. Lett.* **63**, 3230 (1993).
- ⁶D. A. Broido and T. L. Reinecke, *Phys. Rev. B* **51**, 13 797 (1995).
- ⁷S. Y. Ren and J. D. Dow, *Phys. Rev. B* **25**, 3750 (1982).
- ⁸O. S. Gorea, O. M. Tatarinskaya, and A. S. Keyanu, *Three Phonon Scattering in Superlattices*, in 1995 International Semiconductor Conference, CAS'95 Proceedings (Cat. No. 95TH8071), Sinaia, Romania, 1995 (IEEE, New York, 1995), pp. 415–418.
- ⁹P. Hyldgaard and G. D. Mahan, *Phys. Rev. B* **56**, 10 754 (1997).
- ¹⁰X. Y. Zheng, S. Z. Li, M. Chen, and K. L. Wang, in *Micro-Electro-Mechanical Systems (MEMS): Microscale Thermal Phenomena in Electronic Systems*, Proceedings of ASME International Mechanical Engineering Congress and Exposition (ASME, New York, 1996), pp. 93–98.
- ¹¹J. E. Parrott and A. D. Stuckes, *Thermal Conductivity of Solids* (Methuen, New York, 1975).
- ¹²P. G. Klemens, in *Solid State Physics*, edited by F. Seitz and D. Turnbull (Academic, New York, 1958), Vol. 7, p. 1.
- ¹³Y.-J. Han and P. G. Klemens, *Phys. Rev. B* **48**, 6033 (1993).
- ¹⁴J. Callaway, *Phys. Rev.* **113**, 1046 (1959).
- ¹⁵N. Bannov, V. Aristov, and V. Mitin, *Phys. Rev. B* **51**, 9930 (1995).
- ¹⁶A. Svizhenko, A. Balandin, S. Bandyopadhyay, and M. A. Stroschio, *Phys. Rev. B* **57**, 4687 (1998).
- ¹⁷SeGi Yu, K. W. Kim, M. A. Stroschio, G. J. Iafrate, and A. Ballato, *Phys. Rev. B* **50**, 1733 (1994); SeGi Yu, K. W. Kim, M. A. Stroschio, and G. J. Iafrate, *ibid.* **51**, 4695 (1994).
- ¹⁸C. Herring, *Phys. Rev.* **95**, 954 (1954).
- ¹⁹G. Slack, *Phys. Rev.* **105**, 829 (1957).
- ²⁰Yonho S. Ju and K. E. Goodson, *Jpn. J. Appl. Phys., Part 2* **36**, L798 (1997).
- ²¹Yu. Boikov, B. M. Goltsman, and V. A. Danilov, *Semiconductors* **29**, 464 (1995).
- ²²A. Balandin and K. L. Wang, *Bull. Am. Phys. Soc.* **43** (1), 80 (1998).